Journal of Solid State Chemistry 182 (2009) 2402–2408

Contents lists available at ScienceDirect

Journal of Solid State Chemistry

journal homepage: www.elsevier.com/locate/jssc

Determination of the bond-angle distribution in vitreous B_2O_3 by ^{11}B double rotation (DOR) NMR spectroscopy

I. Hung [a,1], A.P. Howes [a], B.G. Parkinson [a], T. Anupõld [b], A. Samoson [b], S.P. Brown [a], P.F. Harrison [a], D. Holland [a,*], R. Dupree [a,*]

[a] Department of Physics, University of Warwick, Coventry CV4 7AL, UK
[b] National Institute for Chemical Physics and Biophysics, Akadeemia Tee 23, Tallinn, Estonia

ARTICLE INFO

Article history:
Received 14 April 2009
Received in revised form
11 June 2009
Accepted 17 June 2009
Available online 23 June 2009

Keywords:
^{11}B DOR
MQDOR
NMR
Spin-diffusion
B_2O_3
Glass

ABSTRACT

The B–O–B bond angle distributions for both ring and non-ring boron sites in vitreous B_2O_3 have been determined by ^{11}B double rotation (DOR) NMR and multiple-quantum (MQ) DOR NMR. The $[B_3O_6]$ boroxol rings are observed to have a mean internal B–O–B angle of $120.0\pm0.7^\circ$ with a small standard deviation, $\sigma_R = 3.2\pm0.4^\circ$, indicating that the rings are near-perfect planar, hexagonal structures. The rings are linked predominantly by non-ring $[BO_3]$ units, which share oxygens with the boroxol ring, with a mean B_{ring}–O–$B_{non\text{-}ring}$ angle of $135.1\pm0.6^\circ$ and $\sigma_{NR} = 6.7\pm0.4^\circ$. In addition, the fraction of boron atoms, f, which reside in the boroxol rings has been measured for this sample as $f = 0.73\pm0.01$.

1. Introduction

Glasses are amorphous, i.e., they possess no long-range order such as is found in crystalline materials, but can be characterised by the short-range order (SRO) imposed by chemical bonding preferences of the constituent atoms. The SRO is defined by the distribution of interatomic distances and bond angles. The former can be determined by diffraction techniques if the system is simple, but information on bond angle distributions, which are also important indicators of the presence of intermediate range order (IRO), are more difficult to extract [1]. In oxide glasses, there has been some success at relating NMR chemical shift distributions to the distribution of the mean M–O–M bond angle [2–5]. Recently the converse has also been reported, i.e., the prediction of the NMR spectrum on the basis of bond angle distributions derived from molecular dynamics (MD) simulations of glass structures [6,7]. In this paper, the first measurement of the effect of the IRO on the B–O–B bond angle distribution in vitreous boron oxide (v-B_2O_3) is reported.

Despite its chemical simplicity, there is continuing debate over the description of the atomic distribution in v-B_2O_3. The suggested presence of significant IRO, in the form of planar six-membered rings (Fig. 1, left-hand inset), is counter-intuitive to the classical description of glass structure as one which possesses SRO only. B_2O_3 is also a structural conundrum because of its remarkable glass-forming ability and reluctance to crystallise. Crystallisation from the melt is not observed at one atmosphere pressure [8], regardless of how slow the cooling rate is and even with use of a crystal seed [9]. It is only possible to produce the crystalline form (B_2O_3-I) from the glass by applying pressure (>4 kbar, $>210\,^\circ$C) [10]. The generally accepted cause of this behaviour is the fact that the structures of the crystal and glass/melt are so dissimilar that there is insufficient energy available to achieve the necessary structural rearrangement on cooling through the liquidus or on reheating the glass at ambient pressure. The large difference in the structures is reflected by their density (glass: 1.81 g cm^{-3} and crystal: 2.46 g cm^{-3}). In crystalline B_2O_3-I, the basic structural unit is a $[BO_3]$ planar triangle, which is connected to other units to form chains [10,11]. On the other hand, the body of evidence for the glassy form supports a structure in which, whilst all boron atoms are still in planar $[BO_3]$ units, a proportion of them are connected via oxygen atoms to give planar, 6-membered $[B_3O_6]$ rings, containing three boron atoms and three oxygen atoms, with three other oxygen atoms acting as links between the boron atoms and the rest of the network. These units (boroxol rings) could be

* Corresponding authors. Fax: +44 2476 150897 (D. Holland); fax: +44 2476 150954 (R. Dupree).
E-mail addresses: D.Holland@warwick.ac.uk (D. Holland), ray.dupree@warwick.ac.uk (R. Dupree).
[1] Present address: CIMAR, National High Magnetic Field Laboratory, Tallahassee, FL 32310, USA.

0022-4596/$ - see front matter © 2009 Elsevier Inc. All rights reserved.
doi:10.1016/j.jssc.2009.06.025

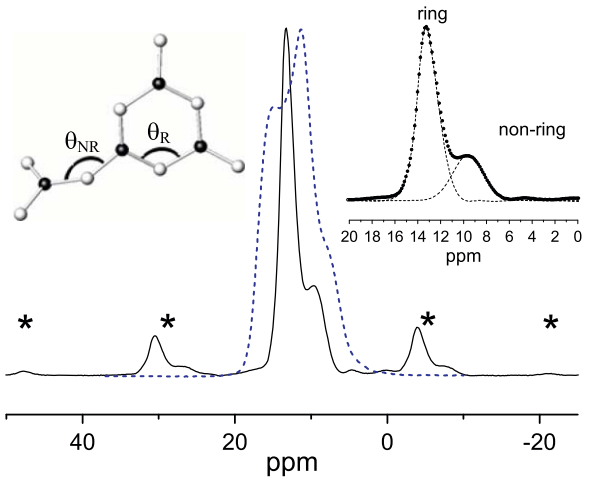

Fig. 1. Double rotation ^{11}B NMR spectrum of vitreous B_2O_3 at 14.1 T. Features labelled * are spinning sidebands separated from the centreband by $2n$ times the spinning frequency (1664 Hz) of the outer DOR rotor. Smaller features in the baseline are due to imperfectly suppressed sidebands corresponding to $(2n+1)$ times the spinning frequency. Superimposed is the centreband of the corresponding one-pulse MAS NMR spectrum (dashed) to indicate the narrowing and enhanced resolution of the spectrum when DOR is used. Right hand inset shows an expansion of the centreband peaks (dots) and the fits (dashed) used for calculating f. Left hand inset shows a schematic of a boroxol ring and one of the linking $[BO_3]$ units; the ring and non-ring B–O–B bond angles are also indicated.

connected to each other either directly (via B–O bonds) or linked by other non-ring $[BO_3]$ units (Fig. 1, left-hand inset). The B–O–B bond angle distribution is a direct measure of the structural disorder of the material, and would reflect the presence of IRO, as well as the occurrence of well-defined rings. The presence of both planar $[B_3O_6]$ rings and connecting $[BO_3]$ units provides a distinctly different B–O–B bond angle distribution from that of a network containing only randomly connected $[BO_3]$ planar triangles. By using double angle rotation (DOR) nuclear magnetic resonance (NMR), the first determination of the bond angle distributions for the ring and non-ring sites in vitreous B_2O_3 are presented herein. This is important information for modelling the structure of glasses, since atomic configurations generated from models can be characterised by their bond angle distributions.

The proportion of boron atoms which are in boroxol rings, f, is a key feature of the v-B_2O_3 structure and its value has been under much debate in the literature. Various experimental data have been reported and models proposed which yield values of f from 0 to 1. Goubeau and Keller [12] suggested the presence of boroxol rings in v-B_2O_3 in order to explain the sharp, highly polarised line at 808 cm^{-1} in the Raman spectrum. This was supported by further Raman studies [13], where isotope substitution confirmed that the sharp peak at 808 cm^{-1} is due to the breathing mode of the oxygen atoms in the ring. However, lack of knowledge of the oscillator strength of the vibration means that the number of boroxol rings in B_2O_3 could not be determined. Early X-ray diffraction studies [14] confirmed the presence of the $[BO_3]$ unit but did not have the sensitivity or resolution to detect the boroxol rings. Careful neutron scattering experiments [15] produced data (both diffraction and inelastic scattering) which could be best fitted with models taking a value for f of 0.8 ± 0.05 (diffraction) and 0.75 (inelastic). In both of these cases, the value of f is not obtained directly from the data but by simulation and comparison. In the present DOR study, a *direct* determination of f is obtained.

NMR can give a direct measure of the fraction of atoms in a given site in a glass. Bray and co-workers [16] used continuous-wave, static ^{10}B, ^{11}B and ^{17}O NMR to show that there are two boron sites and two or more oxygen sites in v-B_2O_3. They deduced a value for f_O (fraction of oxygen atoms in boroxol rings) of approximately 0.55, which equates to a value for f_B of 0.82 in the boroxol ring model described above. The use of magic angle spinning (MAS) NMR, particularly at high magnetic fields and high spinning speeds, makes it easier to observe and quantify the two peaks in the ^{11}B spectrum, although second-order quadrupole effects mean that the lines are complex, broadened and overlap to an extent which causes a certain degree of ambiguity in lineshape fitting and quantification of the two contributing sites. In recent years, values of f obtained using NMR techniques have been reported with values ranging from 0.66 to 0.75 [17–21].

Techniques have been developed which remove the quadrupole contribution to the NMR lineshape and improve resolution. Multiple quantum (MQ) MAS NMR [22] is not readily quantifiable whilst dynamic angle spinning (DAS) NMR [23,24] and double rotation (DOR) NMR [25] are mechanically demanding but can produce quantitative results. Early DOR probes could not achieve the outer rotor spinning speeds necessary to resolve the non-ring peak of v-B_2O_3 from the spinning sidebands [26]. DAS spectra of v-B_2O_3, isotopically dilute in ^{11}B, were obtained at different fields and yielded two peaks in the ratio 3:1 [21]. This ratio is consistent with a model where boroxol rings are linked to each other by non-ring $[BO_3]$ units with which they share oxygens. Thus the more intense peak was assigned to boron atoms in the boroxol ring (B_R) and the smaller peak to non-ring $[BO_3]$ units (B_{NR}) which link the rings. However, this is *not direct evidence* of boroxol rings. Joo et al. [17] approached this by comparing the rates of growth of off-diagonal intensity in spin-diffusion ^{11}B off-MAS NMR experiments on vitreous and crystalline B_2O_3 to identify contributions from co-planar boron atoms (i.e., presumed to be in rings) and non-co-planar boron atoms in the $[BO_3]$ linking units. By this means, they obtained a value for f of 0.66 ± 0.02.

The existence of a planar boroxol group implies some form of stabilisation, possibly aromaticity by delocalised π-bonding. However, a recent neutron diffraction study of crystalline caesium enneaborate, where two thirds of the boron atoms are in boroxol rings and the remainder in triborate groups (like boroxol rings but with one boron atom per ring being 4-coordinated) showed that the B–O distances within the boroxol rings are larger than those which connect the rings, inconsistent with the presence of π-bonding [27].

In addition to experimental determinations of the value of f, there have been numerous attempts at modelling the structure, mostly using molecular dynamics (MD) simulations [28]. Early attempts produced models with very low values of f and also with unrealistic B–O–B bond angles and high density values. The introduction of many-body constraints into the models did generate boroxol rings but with relatively low abundance ($f\sim0.1$) [29,30]. In a recent report of a first-principles MD simulation [6], Umari and Pasquarello (UP) obtained a similar value for f but stressed that the rapid 'quench rate' of MD simulations would not be expected to generate the correct number of boroxol rings although the local configurations could still be employed to simulate data from various experimental techniques if their concentrations were scaled to be consistent with the value of f (0.75) from NMR measurements. This was successfully done for the neutron structure factor of B_2O_3, the neutron density of states, infrared and Raman spectra. Their procedure received critical comment with respect to the simple scaling which ignores the effect which this has on the density [31]. UP responded [32] by pointing to their effective simulation of an ^{11}B NMR isotropic chemical shift spectrum from vitreous B_2O_3 [6]. UP calculated the ^{11}B NMR isotropic chemical shifts, using the method of Sebastiani and Parrinello [33], for the various boron environments generated

by their model and showed that the shift is linearly dependent on the average B–O–B angle for each boron environment. The data were then used to simulate the isotropic ^{11}B NMR spectrum which would be obtained if both dipolar and quadrupolar broadening were eliminated and there was no quadrupolar contribution to the position, i.e., a spectrum arising purely from chemical shift. However, the lineshape under conventional MAS NMR is affected by second-order quadrupole broadening, so a direct comparison with experiment could not be made. The DAS spectrum obtained by Youngman et al. [21] resolved the two sites but still included the quadrupolar-induced shift so that, once again, direct comparison could not be made. Ferlat et al. [7] recently reported a first principles MD calculation to compare the effectiveness of boroxol-rich [34] and boroxol-poor models in simulating experimental structural data. A ^{11}B DAS NMR spectrum and an ^{17}O MAS NMR spectrum were reasonably simulated *only* by the boroxol-rich model.

Double rotation [25,26], which involves simultaneous spinning of the sample at the 'magic angle' (54.74°) *and* at an angle which cancels the $P_4(\cos\theta)$ dependence of second-order quadrupolar broadening (30.56°), was employed to obtain an ^{11}B NMR spectrum of v-B_2O_3 which is free of quadrupolar and dipolar broadening and thus allows a direct determination of f. In addition, by using multiple quantum (MQ) DOR [35–37] to completely separate the chemical shift and quadrupolar effects of the NMR spectrum, a direct comparison can be made with the Umari and Pasquarello simulation [6] and the B–O–B bond angle distribution derived.

2. Experimental procedure

The sample of v-B_2O_3 was prepared by melting B_2O_3 powder in a 90Pt/10Rh crucible at 1000 °C for 20 min followed by quenching of the base of the crucible in water. The resulting glass was removed from the crucible and powdered in a nitrogen glove-box prior to loading into the DOR rotor.

^{11}B DOR NMR experiments were carried out on a Bruker Avance II+ operating at 192.4 MHz ($B_0 = 14.1$ T) and using a DOR probe constructed in Tallinn. A 'selective' $\pi/2$ pulse of 3.75 μs was employed with a recycle delay of 3.0 s. In the experiments performed here the outer rotor speed was 1664 Hz. For the 2D spin-diffusion experiments [38,39] (Fig. 2(a)), the spectral width was 10 kHz in both dimensions with 32 acquisitions per t_1 increment. A standard 3-pulse z-filtered MQMAS pulse sequence [40,41] was employed for the acquisition of the 2D ^{11}B MQDOR spectrum along with a 1.0 s recycle delay (Fig. 2(b)). Pulse widths of 14.5, 4.0 and 20.0 μs with rf fields of 37.1, 37.1 and 6.3 kHz were used for the 3Q excitation, 3Q conversion and read-out pulses, respectively. In addition, 288 transients were acquired for each t_1 increment using spectral widths of 6.4 and 28.8 kHz along F_2 and F_1, resulting in a total experimental time of ~11.2 h; the spectrum was processed using the States method [42] to achieve sign discrimination in F_1. Odd-order spinning sideband suppression was employed for both 1D and 2D spectra [43,44].

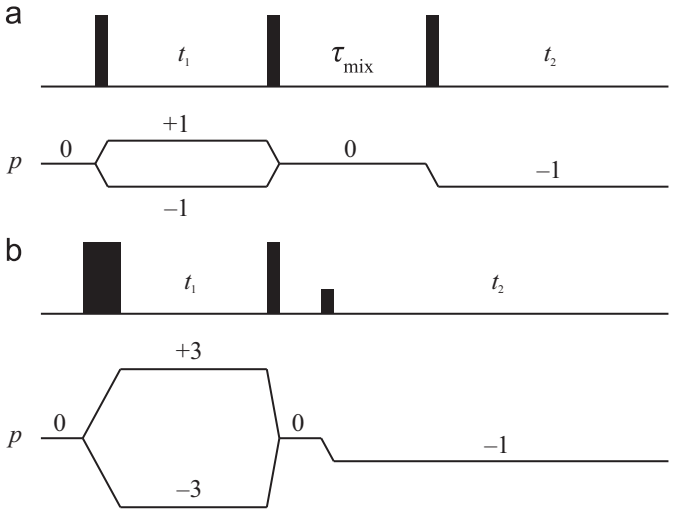

Fig. 2. Pulse sequence and coherence transfer pathway diagrams for (a) the spin-diffusion DOR and (b) the multiple-quantum DOR experiments.

3. Results and discussion

3.1. Ring boron quantification

An ^{11}B DOR spectrum from v-B_2O_3 is shown in Fig. 1. The corresponding one-pulse MAS NMR spectrum is superimposed in order to show the enhanced resolution and hence simplification which is obtained using DOR. An expanded view of the centreband is shown in the right hand inset. The individual peaks are well-resolved and simple peak fitting procedures give direct and unequivocal quantification of the fraction of boron atoms in the ring and non-ring sites. The contributions from these sites have been determined by fitting a Gaussian distribution to the symmetric peak at ~9 ppm and subtracting this from the spectrum to obtain the intensity of the asymmetric peak at ~13 ppm. From the intensities of the centreband *and* the spinning sidebands a ratio for the two sites of 73:27 (each ±1) is obtained, giving $f = 0.73 \pm 0.01$. (It should be noted that there are small features in the baseline from the incompletely suppressed odd-order sidebands. These have been included in the fitting procedure but excluded from the calculation of f, leading to an accuracy of 1%.)

Although it has generally been assumed that the more intense NMR signal comes from [B_3O_6] rings, there is little direct evidence for this. Dipolar-coupling mediated correlation of nuclear spins is widely used for spin $I = \frac{1}{2}$ nuclei. We have recently shown that it is also possible under DOR to assign aluminium ($I = \frac{5}{2}$) sites in a crystalline compound by this method [39]. In this 2D experiment, magnetisation is stored along I_z for a mixing time τ_{mix} and is transferred between dipolar-coupled nuclei when they are strongly coupled (close in distance) giving rise to cross-peaks in the 2D contour plot, while weakly coupled (far apart) nuclei show less intense or non-existent cross-peaks thus revealing the relative proximities of the atoms. Fig. 3 shows spin-diffusion (SD) DOR NMR spectra of v-B_2O_3 taken (using the pulse sequence in Fig. 2(a)) at $\tau_{mix} = 1.0$ and 50.0 ms. At $\tau_{mix} = 1.0$ ms, the signal from the boron atoms with shifts centred at ~9 ppm forms a narrow ridge of intensity, whilst that from the boron atoms at ~13 ppm has spread slightly showing that there is some magnetisation exchange between these atoms, suggesting that they are in close proximity [38,39]. No cross-peak between the two sets of boron atoms is observable on the contour plot at this mixing time. At $\tau_{mix} = 50.0$ ms, the ridge centred at 9 ppm is only slightly broader; however, the 13 ppm peak has spread considerably and there are cross-peaks, showing that the two sets of boron atoms are in reasonably close proximity. This connectivity is further illustrated by Fig. 4, which shows slices taken through the $\tau_{mix} = 50.0$ ms 2D SDDOR spectrum at different F_1 shifts, where the cross-peaks can be clearly seen (e.g. see slice at $F_1 = 9.3$ ppm). Slices near the centre of gravity for each site are also shown for $\tau_{mix} = 1.0$ ms. It is clear that there is little broadening of the line centred at $F_1 = 9.3$ ppm, but there is significant broadening of the $F_1 = 13.3$ ppm resonance, confirming

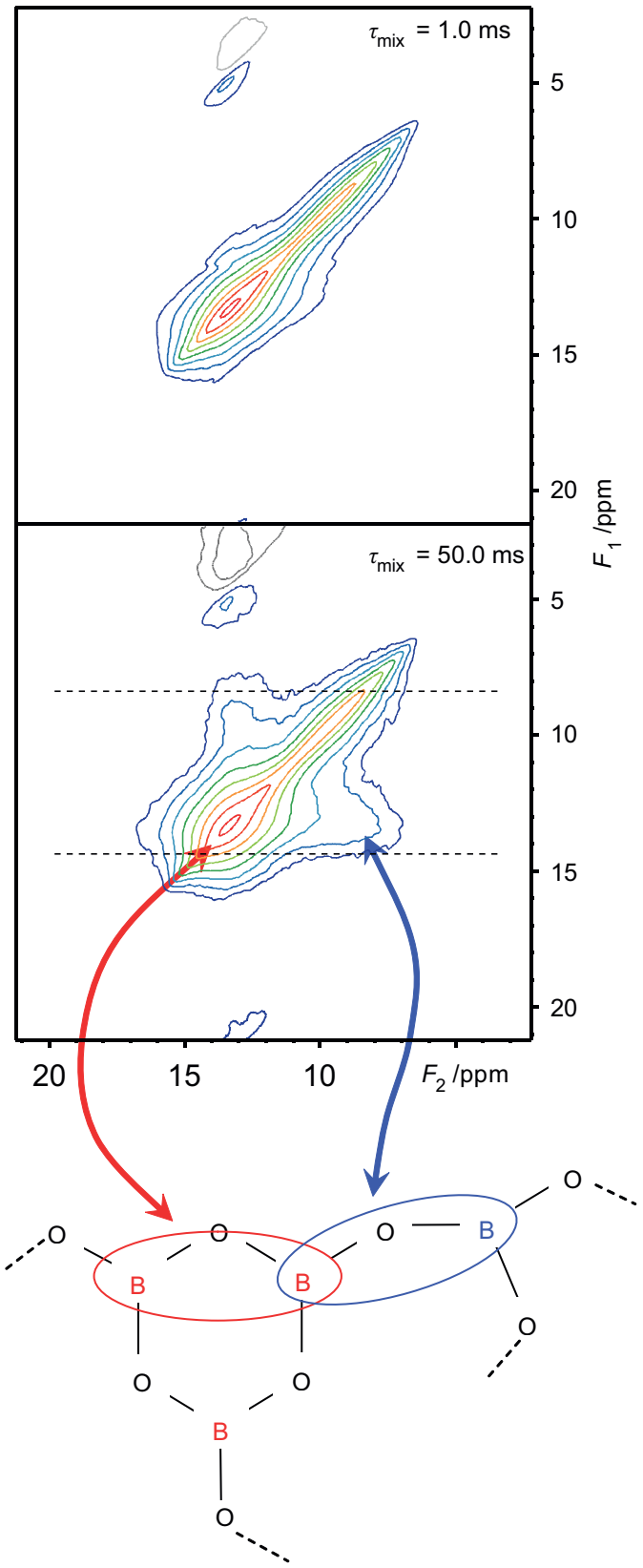

Fig. 3. 2D ^{11}B spin-diffusion DOR NMR spectra of v-B_2O_3 taken using 1.0 and 50.0 ms mixing times. The small features above and below the ring peak are from spinning sidebands. The assignment of the spin-diffusion features to specific nuclear pairs is indicated on the molecular diagram.

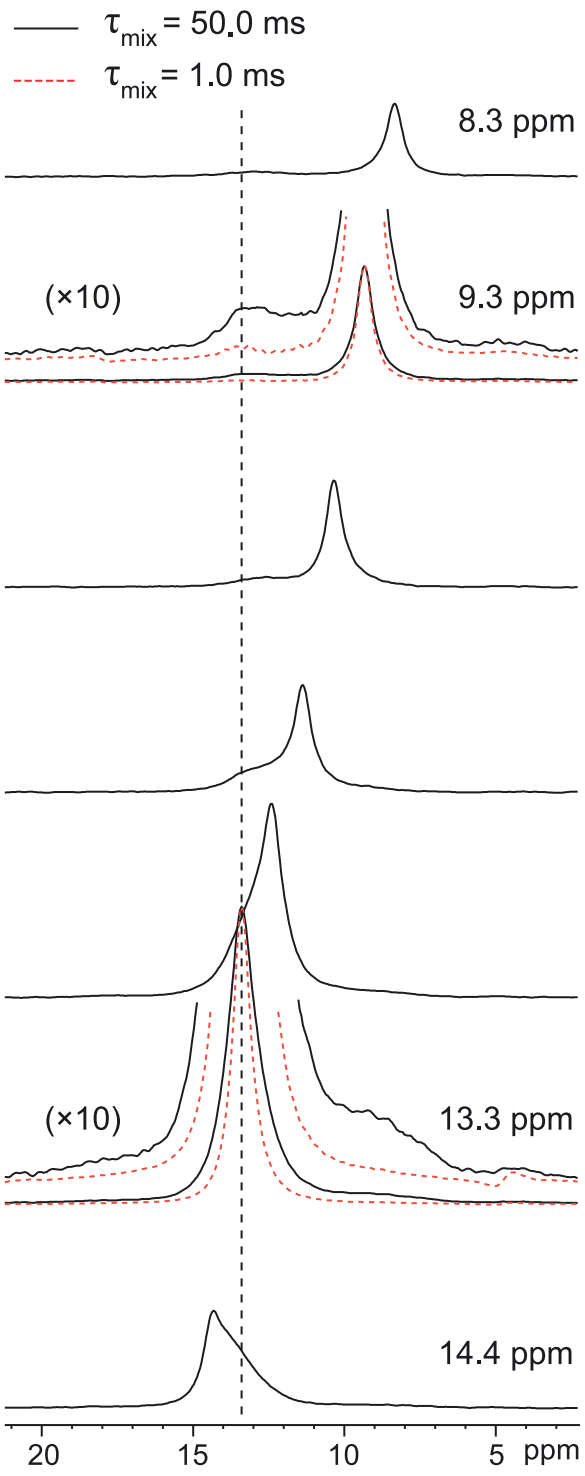

Fig. 4. Slices taken through the 2D spin-diffusion spectrum, between the limits indicated by the dashed lines in Fig. 3. Slices taken from the $\tau_{mix} = 50.0$ ms spectrum are shown as solid lines, whilst the dashed lines are comparisons taken from the spectrum acquired with a mixing time of 1.0 ms.

that boron atoms with this shift are much closer in proximity with each other. Since the ring boron atoms are always adjacent to one another, this is clear evidence that the peak centred near 13 ppm comes from B_R and the peak at 9 ppm is from B_{NR}, which could only be connected to one another in significant numbers if the fraction of boroxol rings was much smaller. Fig. 4 also shows that the position of the cross-peak at 13 ppm is not altered in any of the slices (dashed line), therefore, no particular portion of that peak is

correlated with a specific non-ring component. Thus, since the ^{11}B shift depends on B–O–B angle (as shown by UP), there is no preference for association of specific ring B–O–B angles with specific non-ring B–O–B angles, i.e., the value of one angle does not constrain the value of the other.

With an error in the B_R:B_{NR} ratio of $\pm 1\%$ there is still the possibility that there is some deviation from the 'ideal' arrangement of boroxol rings linked by non-ring [$B_{NR}O_3$] units. There could be [$B_{NR}O_3$]–[$B_{NR}O_3$] links and even some direct ring–ring links (via oxygen), as suggested by Youngman et al. [45]; however, if there were large scale phase separation as proposed by them, then significant B_{NR} to B_{NR} cross-peaks would be observed and B_R to B_{NR} cross-peaks would be much less intense or not visible. Note that, for a value of $f = 0.73 \pm 0.01$, there will be $10 \pm 1\%$ [$B_{NR}O_3$]–[$B_{NR}O_3$] links between rings which might contribute to the slight spread in intensity of the B_{NR} ridge in the SDDOR spectrum at $\tau_{mix} = 50.0$ ms. A recent ^{17}O DOR study of v-B_2O_3 has also shown that there is little or no evidence of [BO_3]–[BO_3] linkages [46].

3.2. B–O–B bond angle distribution

The DOR shift, δ_{DOR}, is related to the isotropic chemical shift for ^{11}B ($I = \frac{3}{2}$) by

$$\delta_{iso} = \delta_{DOR} + \delta_{QIS} = \delta_{DOR} + \frac{1}{40}\frac{C_Q^2}{\nu_0^2}\left(1 + \frac{\eta^2}{3}\right),$$

where C_Q is the quadrupole coupling constant, η is the asymmetry parameter and ν_0 the Larmor resonance frequency. Within error, all of the measurements of C_Q and η in the literature for v-B_2O_3 give very similar values for both B_R and B_{NR} ($C_Q = 2.6$–2.7 MHz; $\eta = 0.16$–0.25) [19–21] so that the quadrupole shift δ_{QIS} is ~4.9 ppm. To obtain more precise values for δ_{QIS} and thus δ_{iso} for the different sites, a 2D MQDOR experiment was carried out [35]. This enables chemical shift and quadrupolar effects on the spectrum to be separated and the true chemical shift distribution to be obtained [47]. The MQDOR spectrum of v-B_2O_3 is shown in Fig. 5. The vertical axis shows the quadrupole shift (which is centred at around 4.95 ppm for the ring sites) and the horizontal axis the chemical shift. Also shown is the summed projection of the 2D spectrum on the isotropic chemical shift axis, i.e., the true chemical shift free of quadrupole effects. Note that, for the non-ring sites, there is a significant slope in the contour lines, i.e., the chemical shift and electric field gradient are correlated, whereas for the ring sites there is a much smaller variation of electric field gradient with shift.

Fig. 6 shows the summed projection from which the average B–O–B bond angle ($\overline{\theta}$) distribution can be extracted using the bond angle/chemical shift relation $\overline{\theta} = 170.6 - 2.55^{\circ}\delta_{iso}$ obtained from UP [6] after shifting by 18.19 ppm from their arbitrary zero. The average bond angle, $\overline{\theta}$, is the average of the three B_X–O–B angles in the coordination of atom B_X. For B_R, $\overline{\theta}_R$ is the average of the two B_R–O–B_R and one B_R–O–B_{NR} angles; for B_{NR}, $\overline{\theta}_{NR}$ is the average of three B_{NR}–O–B_R angles. The distribution of average B–O–B angles was obtained by fitting the spectrum using a Gaussian lineshape for the B_{NR} peak; however, the B_R peak is not Gaussian, being narrower on the small angle side presumably because angles $<120^{\circ}$ are less energetically favourable. This peak could be fitted reasonably well with a bi-Gaussian lineshape. The MQ NMR spectral intensity is not completely quantitative since MQ excitation is dependent on the magnitude of the quadrupolar interaction. However, the average quadrupole interaction constants ($P_Q = C_Q\sqrt{1 + \eta_Q^2/3}$) of the B_R and B_{NR} sites are only slightly different ($P_Q = 2.68$ and 2.61 MHz, respectively) and calculations show that the effect of this will be to reduce the relative intensity of the ring peak slightly, from 0.73 to 0.71, without affecting the shape to within the error arising from the signal-to-noise. The intensities of the two lines were therefore constrained in the fit, which is shown in Fig. 6, to correspond to $f = 0.71$. It should also be noted that the MQDOR spectrum has significant spinning sidebands whose presence contributes to the uncertainty in the relative intensity of the two peaks. However, as differences in both the quadrupolar and shielding parameters are very small, the distribution of intensity into the ssbs should be very similar (if not the same) for the two sites (note this is not a problem for the estimation of f from the DOR spectrum where we have incorporated the sideband intensity in the calculation). The B_R and B_{NR} peak positions (c.o.g. for the bi-Gaussian) are 17.9 ± 0.1 and 13.9 ± 0.2 ppm, respectively, which correspond to average bond angles $\overline{\theta}_R = 125.0 \pm 0.3^{\circ}$ and $\overline{\theta}_{NR} = 135.1 \pm 0.6^{\circ}$ which, as UP point out [6], yields $\overline{\theta}_R \approx (240 + \overline{\theta}_{NR})/3$. Their equation assumes

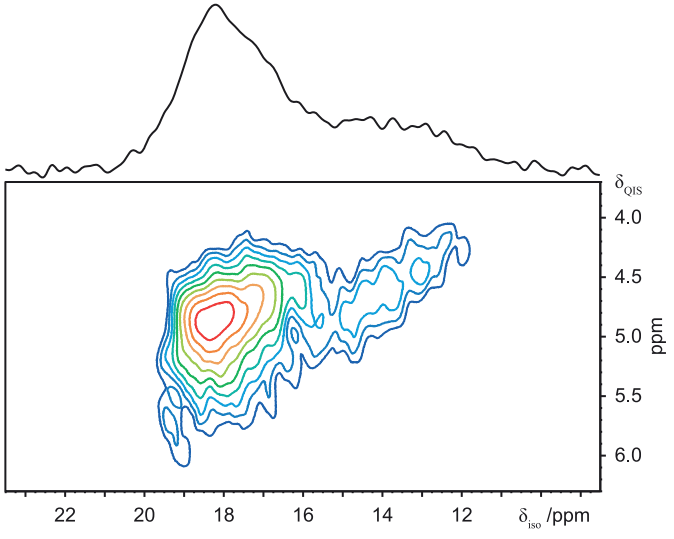

Fig. 5. Multiple quantum DOR ^{11}B NMR spectrum of vitreous B_2O_3. The chemical shift, δ_{iso}, is shown along the horizontal axis and the quadrupolar shift, δ_{QIS}, on the vertical axis. The summed projection of the 2D plot is shown above.

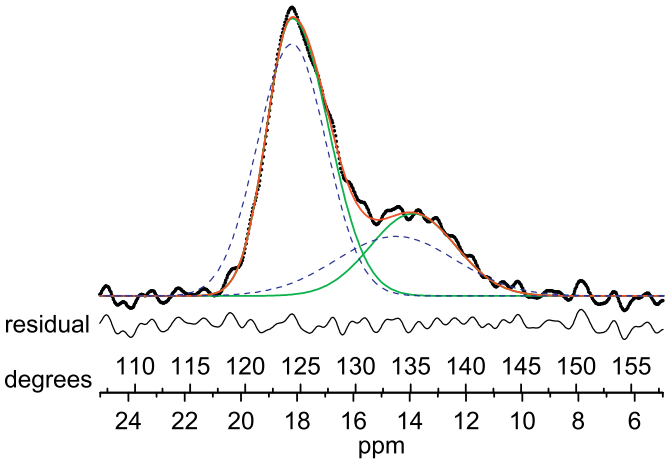

Fig. 6. Comparison of ^{11}B MQDOR shift and bond angle distributions for v-B_2O_3 with the simulation of Umari and Pasquarello [6]. The distributions of mean B–O–B bond angle per boron, for the ring and non-ring sites, are obtained from the MQDOR data by means of the linear relation ($\theta = 170.6^{\circ} - 2.55^{\circ}\delta_{iso}$) between angle, θ, and chemical shift, δ_{iso}. Points represent MQDOR NMR data. Solid lines show a Gaussian fit of the non-ring site centred at ~135° and a bi-Gaussian fit of the ring site at ~125°. The UP simulations, shown with dashed lines, have been shifted by 18.19 ppm and have been scaled to have the same integrated area and ratio as the experimental spectrum.

that the average sum of two B_R–O–B_R angles (θ_R^{AV}) is 240°, indicative of a planar boroxol ring with internal angles of 120°. If we set $\overline{\theta}_R = (2\theta_R^{AV} + \overline{\theta}_{NR})/3$, where θ_R^{AV} refers to the average of the distribution of individual B_R–O–B_R bond angles, then, using the values obtained here, $\theta_R^{AV} = 120 \pm 0.7°$.

The Gaussian fit to the B_{NR} peak of the MQDOR spectrum has a standard deviation, $\overline{\sigma}_{NR}$, of $3.9 \pm 0.2°$ (equivalent to a full-width at half-maximum (FWHM) of 9.2°). Since the B–O–B angle distributions in question are those for the average of three B–O–B angles associated with each boron atom, the B_{NR} distribution is given by convolution of the angle distribution (h) for the individual B_{NR}–O–B_{NR} angle with itself twice ($f(3\phi_{NRP}) = h \otimes h \otimes h$). The σ_{NR} for the individual B_{NR} bond angle distribution is then equal to $\sigma_{NR} = \sqrt{3}\overline{\sigma}_{NR} = 6.7 \pm 0.4°$, assuming all three angles can take any value from within the distribution. In the case of the B_R peak, the distribution of the average B–O–B angle is obtained by convolution of the individual distribution, j, once with itself and once with the non-ring distribution ($g(3\phi_{RP}) = j \otimes j \otimes h$). The σ_R for the individual B_R bond angle distribution is then given by

$$\sigma_R = \left[\frac{(3\overline{\sigma}_R)^2 - \sigma_{NR}^2}{2}\right]^{0.5}.$$

The ring peak, obtained by subtraction of the non-ring Gaussian from the MQDOR data, has a standard deviation, $\overline{\sigma}_{NR}$, of $2.7 \pm 0.2°$ giving $\sigma_R = 3.2 \pm 0.4°$. The small value of σ_R shows the rings are nearly perfect, planar hexagons with a spread in angle similar to that of the boroxol rings in crystalline caesium enneaborate [27] where the B_R–O–B_R angles range from 117.9° to 121.9° (average B_R–O–B_R = 120.5°). Caesium enneaborate is the only crystalline compound to contain significant numbers of boroxol rings but there are no linking [BO_3] units.

The UP chemical shift simulations are overlaid with the MQDOR spectrum and best-fit in Fig. 6. It can be seen that there is considerable similarity in lineshape, although the B_R peak in the ^{11}B DOR data is slightly asymmetric. This is most likely because angles smaller than 120° are likely to be much less favoured than those larger than 120° because of the constraint imposed by the ring structure on the potential energy versus angle dependence. The positions and intensity distributions of the non-ring peaks from the MQDOR and the UP simulation are slightly different, with the experimental separation of the ring and non-ring peak maxima being 4.5 ± 0.1 ppm, which is 0.8 ppm (corresponding to ~2°) larger than calculated by UP. The width of the non-ring distribution is somewhat narrower than that calculated by UP. The B–O–B angles measured here, and the difference in shifts of the ring and non-ring boron, are similar to those found by Zwanziger [48] using density functional theory calculations on small clusters.

The standard deviations in the individual B–O–B angle distributions ($\sigma_{NR} = 6.7°$; $\sigma_R = 3.2°$) can also be compared with those reported for other glass-forming oxides. Both SiO_2 and GeO_2 glasses consist of a network of [MO_4] tetrahedra, linked via oxygen atoms. For SiO_2 the value of σ for the distribution of average Si–O–Si angles, obtained from ^{29}Si NMR, ranges from 7.8° to 15.3° (depending on the model used for the angle/shift dependence [2,3]). Values obtained from ^{17}O NMR give the standard deviation in the single M–O–M bond angle distribution directly and do not require deconvolution from the average distribution which is measured by ^{29}Si NMR. Thus a recent ^{17}O DAS NMR study [4] of SiO_2 gave $\sigma = 3.8°$, significantly smaller than the value obtained from ^{29}Si NMR or diffraction measurements. This is similar to the value of σ from ^{17}O NMR for the distribution of Ge–O–Ge angles in GeO_2, 3.0° [5]; however, both are significantly smaller than the 6.7° found here for the non-ring sites in B_2O_3. This presumably reflects the greater constraint on B_R–O–B_{NR} bond angle relaxation exerted by the presence of the boroxol ring. The maximum in the $\overline{\theta}_{NR}$ distribution of B_2O_3 (~135°) lies between that of GeO_2 (~130°) and SiO_2 (in the range 144–151°). The model of Ferlat et al. [7] gave $\overline{\theta}_{NR} \sim 130°$ rather than the 135.1° we find here.

4. Conclusions

We have demonstrated that the [B_3O_6] rings in vitreous B_2O_3 consist of near-perfect, planar hexagons, and are linked predominantly by non-ring [BO_3] units. The fraction of boron atoms forming boroxol rings ($f = 0.73 \pm 0.01$) was measured with high accuracy for our sample. The mean value of the B–O–B angle in the ring is ~120° with a narrow distribution, $\sigma_R = 3.2°$, whilst the B_R–O–B_{NR} angle has a mean of 135.1° and $\sigma_{NR} = 6.7°$. There is no preference for association of specific ring B–O–B angles with specific non-ring B–O–B angles. The standard deviation σ_{NR} is significantly larger than for the T–O–T angles linking tetrahedral units in glasses such as GeO_2 and SiO_2, which indicates that the presence of a ring boron in the B_R–O–B_{NR} linkage limits the ability of this component of the B_2O_3 network to fully relax. It should be noted that the values presented here refer to this specific sample, prepared as described above. Samples of very different thermal history may have different mean bond angles and distributions.

Acknowledgments

This work was supported by EPSRC, BBSRC and the University of Warwick. I.H. and R.D. thank the Leverhulme Trust for funding. B.P. was supported by EPSRC and Nexia Solutions.

References

[1] J. Neuefeind, K.-D. Liss, Ber. Bunsenges. Phys. Chem. 100 (1996) 1341.
[2] R.F. Pettifer, R. Dupree, I. Farnan, U. Sternberg, J. Non-Cryst. Solids 106 (1988) 408.
[3] F. Mauri, A. Pasquarello, B.G. Pfrommer, Y.-G. Yoon, S.G. Louie, Phys. Rev. B 62 (2000) R4786.
[4] T.M. Clark, P.J. Grandinetti, P. Florian, J.F. Stebbins, Phys. Rev. B 70 (2004) 064202.
[5] R. Hussin, R. Dupree, D. Holland, J. Non-Cryst. Solids 246 (1999) 159.
[6] P. Umari, A. Pasquarello, Phys. Rev. Lett. 95 (2005) 137401.
[7] G. Ferlat, T. Charpentier, A.P. Seitsonen, A. Takada, M. Lazzeri, L. Cormier, G. Calas, F. Mauri, Phys. Rev. Lett. 101 (2008) 065504.
[8] D.R. Uhlmann, J.F. Hays, D. Turnbull, Phys. Chem. Glasses 8 (1967) 1.
[9] F.C. Kracek, G.W. Morey, H.E. Merwin, Am. J. Sci. 35A (1938) 143.
[10] G.E. Gurr, P.W. Montgomery, C.D. Knutson, B.T. Gorres, Acta Crystallogr. B 26 (1970) 906.
[11] S.L. Strong, R. Kaplow, Acta Crystallogr. B 26 (1968) 906.
[12] J. Goubeau, H. Keller, Z. Anorg. Allg. Chem. 272 (1953) 303.
[13] C.F. Windisch, W.M. Risen, J. Non-Cryst. Solids 48 (1982) 307.
[14] B.E. Warren, H. Krutter, O. Morningstar, J. Am. Ceram. Soc. 18 (1936) 202.
[15] A.C. Hannon, D.I. Grimley, R.A. Hulme, A.C. Wright, R.N. Sinclair, J. Non-Cryst. Solids 177 (1994) 299.
[16] J.E. Jellison, L.W. Panek, P.J. Bray, G.B. Rouse, J. Chem. Phys. 66 (1977) 802.
[17] C. Joo, U. Werner-Zwanziger, J.W. Zwanziger, J. Non-Cryst. Solids 261 (2000) 282.
[18] C. Joo, U. Werner-Zwanziger, J.W. Zwanziger, J. Non-Cryst. Solids 271 (2000) 265.
[19] S.K. Lee, K. Mibe, Y. Fei, G.D. Cody, B.O. Mysen, Phys. Rev. Lett. 94 (2005) 165507.
[20] S.-J. Hwang, C. Fernandez, J.P. Amoureux, J. Cho, S.W. Martin, M. Pruski, Solid State Nucl. Magn. Reson. 8 (1997) 109.
[21] R.E. Youngman, J.W. Zwanziger, J. Non-Cryst. Solids 168 (1994) 293.
[22] L. Frydman, J.S. Harwood, J. Am. Chem. Soc. 117 (1995) 5367.
[23] A. Llor, J. Virlet, Chem. Phys. Lett. 152 (1988) 248.
[24] K.T. Mueller, B.Q. Sun, G.C. Chingas, J.W. Zwanziger, T. Terao, A. Pines, J. Magn. Reson. 86 (1990) 470.
[25] A. Samoson, E. Lippmaa, Mol. Phys. 65 (1988) 1013.
[26] R.E. Youngman, U. Werner-Zwanziger, J.W. Zwanziger, Z. Naturforsch. 51a (1996) 321.
[27] A.C. Wright, R.N. Sinclair, C.E. Stone, K.S. Knight, I.G. Polyakova, N.M. Vedischeva, B.A. Shakhmatkin, Phys. Chem. Glasses 44 (2003) 197.

[28] W. Soppe, C.v.d. Marel, W.F.v. Gunsteren, H.W.d. Hartog, J. Non-Cryst. Solids 103 (1988) 201.
[29] J. Swenson, L. Borjesson, Phys. Rev. B 55 (1997) 11138.
[30] M. Teter, in: A.C. Wright, S.A. Feller, A.C. Hannon (Eds.), Borate Glasses, Crystals and Melts, Society of Glass Technology, Sheffield, 1997, p. 407.
[31] J. Swenson, L. Borjesson, Phys. Rev. Lett. 96 (2006) 199701.
[32] P. Umari, A. Pasquarello, Phys. Rev. Lett. 96 (2006) 199702.
[33] D. Sebastiani, M. Parrinello, J. Phys. Chem. A 105 (2001) 1951.
[34] A. Takada, C.R.A. Catlow, G.D. Price, Phys. Chem. Glasses 44 (2003).
[35] A. Samoson, J. Magn. Reson. A 121 (1996) 209.
[36] T. Anupold, A. Rheinhold, P. Sarv, A. Samoson, Solid State Nucl. Magn. Reson. 13 (1998) 87.
[37] A.P.M. Kentgens, E.R.H.v. Eck, T.G. Ajithkumar, T. Anupold, J. Past, A. Reinhold, A. Samoson, J. Magn. Reson. 178 (2006) 212.
[38] M. Eden, L. Frydman, J. Phys. Chem. B 107 (2003) 14598.
[39] I. Hung, A. Wong, T. Anupold, A. Samoson, M.E. Smith, S.P. Brown, R. Dupree, Chem. Phys. Lett. 432 (2006) 152.
[40] J.P. Amoureux, C. Fernandez, S. Steuernagel, J. Magn. Reson. Ser. A 123 (1996) 116.
[41] M. Hanaya, R.K. Harris, J. Phys. Chem. A 101 (1997) 6903.
[42] D.J. States, R.A. Haberkorn, D.J. Ruben, J. Magn. Reson. 48 (1982) 286.
[43] A. Samoson, J. Tegenfeldt, J. Magn. Reson. Ser. A 110 (1994) 238.
[44] A. Samoson, T. Anupold, Solid State Nucl. Magn. Reson. 15 (2000) 217.
[45] R.E. Youngman, S.T. Haubrich, J.W. Zwanziger, M.T. Janicke, B.F. Chmelka, Science 269 (1995) 1416.
[46] A. Wong, A.P. Howes, B.G. Parkinson, T. Anupõld, A. Samoson, D. Holland, R. Dupree, Phys. Chem. Chem. Phys. (2009)10.1039/b906501f.
[47] I. Hung, A. Wong, A.P. Howes, T. Anupõld, A. Samoson, M.E. Smith, D. Holland, S.P. Brown, R. Dupree, J. Magn. Reson. 197 (2009) 229.
[48] J.W. Zwanziger, Solid State Nucl. Magn. Reson. 27 (2005) 5.